



Ising superconductivity and Majorana fermions in transition-metal dichalcogenides

Benjamin T. Zhou, Noah F. Q. Yuan, Hong-Liang Jiang, and K. T. Law*

Department of Physics, Hong Kong University of Science and Technology, Clear Water Bay, Hong Kong, China

(Received 23 October 2015; revised manuscript received 14 March 2016; published 4 May 2016)

In monolayer transition-metal dichalcogenides (TMDs), electrons in opposite K valleys are subject to opposite effective Zeeman fields, which are referred to as Ising spin-orbit coupling (SOC) fields. The Ising SOC, originating from in-plane mirror symmetry breaking, pins the electron spins to the out-of-plane directions, and results in Ising superconducting states with strongly enhanced upper critical fields. Here, we show that the Ising SOC generates equal-spin-triplet Cooper pairs with spin polarized in the in-plane directions. Importantly, the spin-triplet Cooper pairs can induce superconducting pairings in a half-metal wire placed on top of the TMD and result in a topological superconductor with Majorana end states. Direct ways to detect equal-spin triplet Cooper pairs and the differences between Ising superconductors and Rashba superconductors are discussed.

DOI: [10.1103/PhysRevB.93.180501](https://doi.org/10.1103/PhysRevB.93.180501)

Introduction. Monolayer transition-metal dichalcogenides (TMDs) are two-dimensional (2D) materials composed of a layer of triangularly arranged transition-metal atoms sandwiched between two layers of triangularly arranged chalcogenide atoms, forming a 2D honeycomb lattice similar to graphene but with broken sublattice symmetry [1,2]. With their strong mechanical properties, relatively high electron mobility, and a massive Dirac energy spectrum [3,4], monolayer TMDs are considered potential materials for next generation transistors [5–9]. Interestingly, due to the breaking of in-plane mirror symmetry and strong atomic spin-orbit coupling (SOC), electrons near the K and $-K$ valleys are subject to strong effective Zeeman fields [10–14], as depicted in Fig. 1(a). These effective Zeeman fields strongly polarize electron spins to the out-of-plane directions and the spin polarizations are opposite at opposite valleys. To distinguish this special type of SOC from 2D Rashba SOC which pins electron spins to in-plane directions, we refer to this effective Zeeman field as the Ising SOC field.

Even though the normal states of monolayer TMDs have been studied extensively in recent years [15], the experimental [16–22] and theoretical [23–26] studies of the superconducting monolayer TMDs have only just started. It was first shown recently that gated MoS₂ thin films, with conducting electrons trapped in a single layer, exhibit superconductivity at about 10 K with optimal gating [16,17]. Importantly, the in-plane upper critical field H_{c2} of the system can be several times larger than the Pauli limit and an order of magnitude larger than the H_{c2} of bulk superconducting samples where inversion symmetry is restored [19,20]. In recent experiments, monolayers of NbSe₂ have been successfully fabricated, which are superconducting [21], and the in-plane H_{c2} exhibits strong enhancement similar to gated MoS₂ [22].

As explained in Refs. [19,20,22], Ising SOC has opposite directions in opposite valleys so that it preserves time-reversal symmetry and is compatible with superconductivity. Owing to the strong pinning of electron spins to the out-of-plane directions by Ising SOC, external in-plane magnetic fields are much less effective in aligning electron spins. As a result, H_{c2}

is strongly enhanced. We refer to this special type of non-centrosymmetric superconductor as an Ising superconductor [19,22].

In gated MoS₂, the experimental data are well explained by solving the self-consistent gap equation which includes the Ising SOC fields of about 100 T (≈ 6 meV in Zeeman energy) [19,20]. In NbSe₂, the estimated Ising SOC is even larger at about 660 T due to the stronger SOC in the hole bands [22]. Both of the estimations extracted from the MoS₂ and NbSe₂ experiments are consistent with the corresponding Ising SOC found from density functional theory (DFT) calculations [10,12,13].

However, important questions still remain: (1) Besides the in-plane H_{c2} measurements, are there other ways to detect Ising superconductivity? (2) Are there any experimental consequences of Ising superconductivity? This Rapid Communication is devoted to answering these questions.

In the following, we show that Ising SOC induces spin-triplet pairing correlations in an s -wave superconductor. Moreover, spin-triplet Cooper pairs are formed by electrons with equal spins pointing to the in-plane directions. As a result, half-metal leads with spin \mathbf{h} polarized to the in-plane directions can freely tunnel Cooper pairs into the superconductor. The Andreev reflection tunneling amplitude decreases as \mathbf{h} deviates from the in-plane directions. This would give an experimental signature of Ising superconductivity, as depicted in Fig. 2. More importantly, when a half-metal wire is placed on top of the Ising superconductor, spin-triplet pairing can be induced on the wire given that \mathbf{h} has in-plane components. This would result in a one-dimensional (1D) topological superconductor, which supports Majorana end states, as depicted in Fig. 1. Finally, the differences between Ising SOC and Rashba SOC are discussed.

Equal-spin pairing in Ising superconductors. To be specific, we study the properties of Ising superconductivity in monolayer MoS₂ but the conclusion obtained is very general and can be applied to many other superconducting TMD materials with Ising SOC. In recent experiments, electrons of MoS₂ thin films are mostly trapped in the top layer due to heavy liquid gating. The samples exhibit superconductivity when the conduction bands near the K valleys are filled and the T_c is about 10 K at optimal gating [16,17,19,20]. The conduction bands near the K points are predominantly originating from

*phlaw@ust.hk

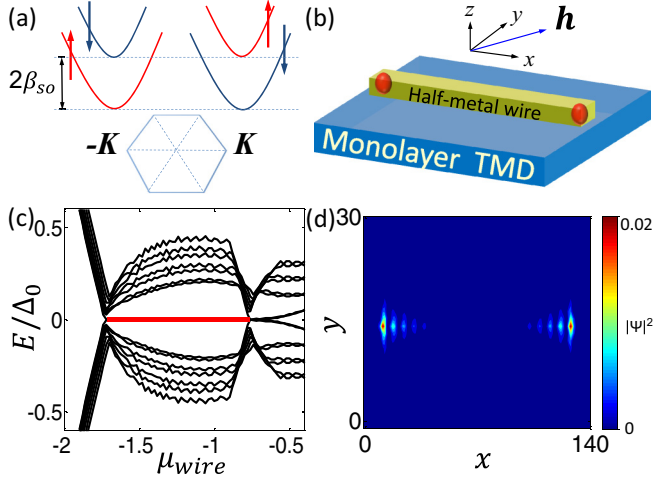


FIG. 1. (a) The electrons near the K and $-K$ valleys subject to the Ising SOC fields in opposite directions. The effective Zeeman gap is $2\beta_{so}$, as defined in Eq. (1). (b) A half-metal wire is placed on top of a superconducting monolayer TMD. Majorana fermions (red dots) appear at the ends of wire when the spin polarization \mathbf{h} of the half metal has in-plane components. (c) The energy spectrum of the setup in (b) as a function of the chemical potential of the wire μ_w , using the tight-binding model in Eq. (8). The red line highlights the topological regime with Majorana modes. (d) The zero energy ground state wave function of the system in the topological regime in (c). Evidently, two Majorana fermions reside at the ends of the wire. The parameters of (c) and (d) are given in the Supplemental Material [29].

the Mo $4d_{z^2}$ orbitals of the triangularly arranged Mo atoms [14,16]. The effective Hamiltonian near the K valleys, in the basis of $(c_{k\uparrow}, c_{k\downarrow})$, can be written as [26]

$$H_0(\mathbf{k} = \mathbf{p} + \epsilon\mathbf{K}) = \left(\frac{|\mathbf{p}|^2}{2m} - \mu \right) \sigma_0 + \epsilon\beta_{so}\sigma_z, \quad (1)$$

where $\mathbf{K} = (4\pi/3, 0)$ is the momentum of the K point, \mathbf{p} denotes the momentum deviated from K or $-K$ points, and $\epsilon = \pm$ is the valley index. The out-of-plane direction is chosen as the z axis. The β_{so} term originates from the coupling between the Mo atoms and the S atoms. As a result, this term breaks the in-plane mirror symmetry. It pins the electron spins to the out-of-plane directions and is referred to as Ising SOC here to distinguish it from the Rashba SOC terms which arise due to mirror symmetry breaking in the out-of-plane direction and pin electron spins to the in-plane directions.

The superconducting MoS₂ with spin-singlet s -wave pairing potential Δ_0 can be described by the following mean field Hamiltonian in the Nambu basis $(c_{k\uparrow}, c_{k\downarrow}, c_{-k\uparrow}^\dagger, c_{-k\downarrow}^\dagger)$:

$$H_{\text{BdG}}(\mathbf{k}) = \begin{pmatrix} H_0(\mathbf{k}) & \Delta_0 i\sigma_y \\ -\Delta_0 i\sigma_y & -H_0^*(-\mathbf{k}) \end{pmatrix}. \quad (2)$$

As demonstrated in the seminal works in Refs. [27,28], the pairing symmetry of the Cooper pairs can be found by solving the Gor'kov equations to obtain the pairing correlations. The pairing correlations are defined as

$$F_{\alpha\beta}(\mathbf{k}, E) = -i \int_0^\infty e^{i(E+i0^+)t} \langle \{c_{k,\alpha}(t), c_{-k,\beta}(0)\} \rangle dt. \quad (3)$$

Using H_{BdG} and expressing the pairing correlations in matrix form, we have

$$F(\mathbf{k}, E) = \Delta_0 [\psi_s(\mathbf{k}, E)\sigma_0 + \mathbf{d}(\mathbf{k}, E) \cdot \boldsymbol{\sigma}] i\sigma_y, \quad (4)$$

where ψ_s parametrizes the spin-singlet pairing correlation and the \mathbf{d} vector parametrizes the spin-triplet pairing. The \mathbf{d} vector is parallel to the z direction in the Ising superconductor case with $\mathbf{d} = (0, 0, d_z)$. Near the K valleys,

$$\psi_s(\mathbf{p} + \epsilon\mathbf{K}, E) = \frac{E_+^2 - \Delta_0^2 - \xi_p^2 - \beta_{so}^2}{M(\mathbf{p}, E_+)}, \quad (5)$$

$$d_z(\mathbf{p} + \epsilon\mathbf{K}, E) = \frac{2\epsilon\beta_{so}\xi_p}{M(\mathbf{p}, E_+)}, \quad (6)$$

where $\xi_p = |\mathbf{p}|^2/2m - \mu$, $M(\mathbf{p}, E) = (\Delta_0^2 + \xi_p^2 - E^2)^2 + 2\beta_{so}^2(\Delta_0^2 - \xi_p^2 - E^2) + \beta_{so}^4$, and $E_+ = E + i0^+$.

It is possible to generalize the pairing matrix of the Hamiltonian in Eq. (2) from $\Delta_0 i\sigma_y$ to $[\Delta_0 + \Delta_r \sigma_z] i\sigma_y$. As shown in Ref. [26], the spin-triplet Δ_r term belongs to the same irreducible representation as the Δ_0 term. Importantly, this Δ_r term does not change the form of the pairing correlation matrix in Eq. (4) but enhances the triplet pairing correlation in Eq. (6). The effect of Δ_r on the pairing correlations is discussed in the Supplemental Material [29].

It is important to note that for small β_{so} the triplet pairing correlation d_z is linearly proportional to β_{so} . As expected, the Ising SOC generates the mixing of spin-singlet and spin-triplet pairings [27,28] even when Δ_r is zero [30]. In the basis where the spin quantization axis is along the out-of-plane directions, only the σ_x, σ_y components of $F(\mathbf{k}, E)$ are nonzero and both the spin-singlet and spin-triplet Cooper pairs are formed by electrons with opposite spins. However, by choosing the new spin quantization axis in the xz plane, which forms an angle θ with the z axis, the pairing correlations become

$$F_\theta(\mathbf{k}, E) = \begin{pmatrix} -d_z \sin \theta & \psi_s + d_z \cos \theta \\ -\psi_s + d_z \cos \theta & d_z \sin \theta \end{pmatrix}. \quad (7)$$

When the spin quantization axis is along the x direction with $\theta = \pi/2$, all the triplet Cooper pairs are formed by equal-spin electron pairs with spins pointing to in-plane directions. In the following, we show that the property of possessing equal-spin-triplet Cooper pairs has important experimental consequences in the detection of Ising superconductivity and the creation of Majorana fermions.

Detecting equal-spin Cooper pairs. As shown in Eq. (7), the equal-spin-triplet pairing correlation is maximum when the spin quantization axis is in plane and zero when the axis is out of plane. When a half-metal lead is attached to the Ising superconductor, as depicted in Fig. 2(a), only equal-spin Andreev reflection processes, which inject equal-spin Cooper pairs into the superconductor, are allowed since all the electrons in the half metal are spin polarized. On the other hand, ordinary Andreev reflection processes which inject spin-singlet Cooper pairs into the superconductor are strongly suppressed. Since the Cooper pairs in the Ising superconductor have spin pointing to in-plane directions, the equal-spin Andreev reflection amplitude is maximum when the spin polarization \mathbf{h} of the half-metal lead is parallel to the in-plane directions. As \mathbf{h} deviates from the in-plane directions,

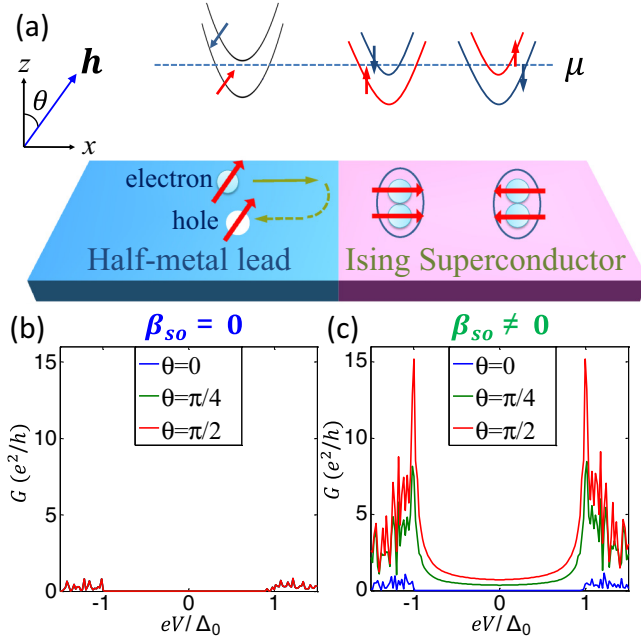


FIG. 2. (a) A half-metal lead is attached to an Ising superconductor. The spin polarization direction of the half metal is \mathbf{h} . Both spin-singlet and spin-triplet Cooper pairs can exist in Ising superconductors due to Ising SOC. Equal-spin-triplet Cooper pairs have electron spins pointing to the in-plane directions. Schematic band structures are shown with the horizontal dashed line representing the chemical potential. (b) and (c) The tunneling conductance at a half-metal/Ising superconductor interface. $\beta_{so} = 0$ in (b) and $\beta_{so} \neq 0$ in (c). In (c), the tunneling conductance decreases when \mathbf{h} deviates from the in-plane directions. The parameters of (b) and (c) are given in the Supplemental Material [29].

the Andreev reflection tunneling amplitude decreases and becomes minimum when \mathbf{h} is perpendicular to the in-plane directions.

The tunneling charge conductance of the half-metal/Ising superconductor junction is shown in Figs. 2(b) and 2(c), in the absence and presence of the Ising SOC terms, respectively. The currents are calculated using the recursive Green's function approach [31,32] based on the tight-binding model H_{TMD} of Eq. (8) discussed below. From Fig. 2(b), it is evident that, when $\beta_{so} = 0$, the in-gap charge conductance is zero. This is due to the suppression of ordinary Andreev reflection in the half-metal lead. When β_{so} is finite, in-gap equal-spin Andreev reflections are possible due to the triplet pairing correlations induced by the Ising SOC and the in-gap conductance is finite. Moreover, the conductance decreases when \mathbf{h} deviates from the in-plane direction ($\theta = \pi/2$) and reaches the minimum when \mathbf{h} is perpendicular to the in-plane directions ($\theta = 0$), as expected.

If a CrO_2 film, which has the magnetic easy axis pointing to the out-of-plane directions, is used as the half-metal lead, the spin polarization of CrO_2 can be continuously tuned to the in-plane directions by a small in-plane magnetic field [33,34] which will not induce any orbital effects on the Ising superconductor.

Majorana fermions in an Ising superconductor. The realization of topological superconductors which support zero energy Majorana bound states has been one of the most important topics in condensed matter physics in recent years [35–38]. One of the most promising ways to realize topological superconductors is to induce pairing by proximity effects on semiconducting wires with Rashba SOC and external magnetic fields [39–47]. Magnetic atomic chains on Rashba superconductors can potentially be used to realize Majorana fermions [48].

Here, we point out that superconducting monolayer TMDs provide an alternative route to realize Majorana fermions. This is due to the fact that in-plane equal-spin-triplet pairing correlations are induced by the Ising SOC. When a half-metal wire is placed on top of the TMD, electrons with the same spin can form pairs, as long as the spin polarization of the electrons is not perpendicular to the plane. The induced pairing gap is largest when the spin polarization in the half-metal wire is aligned to the in-plane directions.

To demonstrate the induced equal-spin pairing effect on the half-metal wire which is in proximity to the TMD, we consider a system as depicted in Fig. 1(b). The system is described by the following tight-binding Hamiltonian H_{tot} ,

$$\begin{aligned}
 H_{\text{tot}} &= H_{\text{TMD}} + H_{\text{wire}} + H_c, \\
 H_{\text{TMD}} &= \sum_{\mathbf{R}, j, s, s'} c_{\mathbf{R}, s}^\dagger \left(\frac{2}{3m} \sigma_0 + i \frac{\beta_{so}}{3\sqrt{3}} \sigma_z \right)_{ss'} c_{\mathbf{R}+\mathbf{r}_j, s'} \\
 &+ \sum_{\mathbf{R}} \Delta_0 c_{\mathbf{R}, \uparrow}^\dagger c_{\mathbf{R}, \downarrow}^\dagger + \text{H.c.} - \sum_{\mathbf{R}, s} \left(\mu - \frac{2}{m} \right) c_{\mathbf{R}, s}^\dagger c_{\mathbf{R}, s}, \\
 H_{\text{wire}} &= \sum_{n, s} -t_w f_{n\mathbf{r}_0, s}^\dagger f_{(n+1)\mathbf{r}_0, s} - \frac{1}{2} \mu_w f_{n\mathbf{r}_0, s}^\dagger f_{n\mathbf{r}_0, s} \\
 &+ \sum_{n, s, s'} f_{n\mathbf{r}_0, s}^\dagger \left(\frac{1}{2} \mathbf{h} \cdot \boldsymbol{\sigma} \right)_{ss'} f_{n\mathbf{r}_0, s'} + \text{H.c.}, \\
 H_c &= \sum_{n, s} -t_c f_{n\mathbf{r}_0, s}^\dagger c_{n\mathbf{r}_0, s} + \text{H.c.}, \tag{8}
 \end{aligned}$$

where $c_{\mathbf{R}, s}$ and $f_{\mathbf{R}, s}$ are electron annihilation operators of the TMD and the wire, respectively. The three lattice vectors of the TMD are denoted as $\mathbf{r}_j = (\cos \frac{2j\pi}{3}, \sin \frac{2j\pi}{3})$ ($j = 0, 1, 2$). The hopping and chemical potential of the wire are denoted as t_w and μ_w , respectively, \mathbf{h} denotes the polarization field in the wire, and t_c is the coupling between the wire and TMD.

In order to make the wire a half metal, we set $|\mu_w + 2t_w| \ll 2|\mathbf{h}|$ and the wire is parallel to the zigzag edge direction of the TMD which is defined as the x direction. The wire can also be placed along any other directions except the armchair direction where the induced triplet pairing is zero.

Due to the translation symmetry along the wire, we can integrate out the superconducting TMD and plot the spectral function $A(k_x, \omega)$ of the half-metal wire where

$$A(k_x, \omega) = \frac{i}{2\pi} \text{tr}[G^R(k_x, \omega) - G^A(k_x, \omega)]. \tag{9}$$

Here, $G^{R/A}(k_x, \omega)$ are the retarded/advanced Green's functions of the wire including the self-energy contribution from the superconducting TMD. As shown in Fig. 3(a), an energy gap

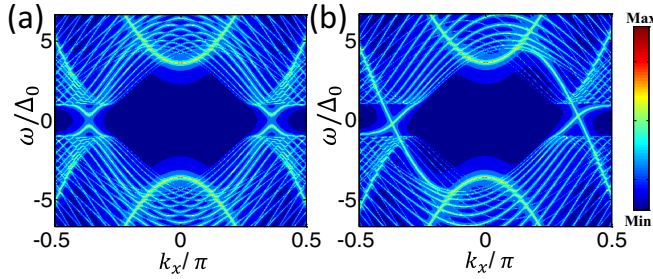


FIG. 3. The spectral function of a half-metal wire in proximity to a monolayer superconducting TMD. (a) The spin polarization \mathbf{h} of the wire is in plane. An energy gap is induced on the wire. (b) \mathbf{h} is perpendicular to the plane. The superconducting TMD cannot induce equal-spin pairing on the wire and the wire is gapless. The parameters of the model are given in the Supplemental Material [29].

opens when the spin polarization \mathbf{h} of the wire is parallel to the in-plane direction. On the contrary, the pairing gap vanishes when \mathbf{h} of the half metal is out of plane, as shown in Fig. 3(b). The energy spectrum of the system as a function of μ_w , with \mathbf{h} pointing to an in-plane direction, is shown in Fig. 1(c). From Fig. 1(c), it is evident that there is a topological regime with zero energy modes. The zero energy ground state wave function for the system in the topological regime is depicted in Fig. 1(d). It is evident that there is a Majorana end state residing at each end of the half-metal wire.

Analytically, after integrating out the TMD background, the effective Hamiltonian H_{eff} of the half-metal wire at zero frequency can be written as

$$H_{\text{eff}}(k_x, \omega = 0) = (-2t_{\text{eff}} \cos k_x - \mu_{\text{eff}})\tau_z + \Delta_{\text{eff}} \sin k_x \tau_x. \quad (10)$$

Here, the basis is $(a_{k_x}, a_{-k_x}^\dagger)$ and a_{k_x} is the annihilation operator of a spin polarized electron in the half-metal wire, $t_{\text{eff}}, \mu_{\text{eff}}$ are effective hopping and effective chemical potential, respectively, and Δ_{eff} represents the equal-spin pairing induced on the wire by the background TMD. It has the form $\Delta_{\text{eff}} \propto Z\Delta_0\beta_{\text{so}} \sin \theta$. This indicates that the Ising SOC term is essential in inducing the pairing on the half-metal wire and \mathbf{h} should have in-plane components as shown Fig. 3. Importantly, H_{eff} is the same as the Kitaev model of a 1D spinless p -wave superconductor [49] which is topologically nontrivial when $|\mu_{\text{eff}}| < 2t_{\text{eff}}$. In other words, the half-metal wire is topological as long as the conduction band is partially occupied. Since the effective Hamiltonian of the system is in the D class [50],

introducing small Rashba SOC into the system [26,51] does not affect the topological phase. It is important to note that Δ_{eff} can be comparable with Δ_0 of the parent superconductor. In the particular calculation in Fig. 3(a), the induced gap is about one third of Δ_0 , which is about 1 meV in superconducting NbSe₂ or NbS₂.

It is important to note that superconducting TMD provides a very practical way to create Majorana fermions. One may place a half-metal wire such as CrO₂ on top of a superconducting TMD as depicted in Fig. 1(b), and then apply an in-plane magnetic field (in any in-plane direction) to align the spins of the half metal. One may also use magnetic atomic chains [48] to replace the half-metal wire. As shown in recent experiments, superconducting TMDs indeed have extremely large in-plane H_{c2} , above 50 T, as shown in Refs. [19,20,22], such that the in-plane magnetic field will not destroy the bulk superconducting properties of the system.

We can now compare Ising superconductors with Rashba superconductors. In 2D Rashba superconductors with a Rashba vector \mathbf{g} , where \mathbf{g} is pointing to the in-plane directions, the induced equal-spin Cooper pairs in Rashba superconductors have spins aligned in the out-of-plane directions [28,29]. When a half-metal wire is placed on top of a Rashba superconductor, a superconducting pairing gap can be induced on the wire when the spin polarization of the wire \mathbf{h} has out-of-plane components. This results in a topological superconductor. However, the induced pairing gap vanishes when \mathbf{h} is in the in-plane direction and perpendicular to the wire. A detailed comparison between Ising and Rashba superconductors can be found in the Supplemental Material [29].

Moreover, Ising SOC in TMD materials is very strong and can cause band splitting of over 100 meV. We believe that, a monolayer or a few layers of NbSe₂ and NbS₂, being intrinsic superconductors with strong Ising SOC in the hole bands [21,22], are particularly promising materials for realizing Majorana fermions.

Conclusion. In this work, we show that Ising SOC induces equal-spin-triplet pairs with electron spins pointing to the in-plane directions. The equal-spin Cooper pairs can be detected in tunneling experiments. Majorana fermions can be created when a half-metal wire is placed on top of a superconducting TMD.

K.T.L. thanks Patrick Lee for illuminating discussions. The authors acknowledge the support of HKRGC and the Croucher Foundation through HKUST3/CRF/13G, 602813, 605512, 16303014, and a Croucher Innovation Grant.

-
- [1] A. Bromley, R. B. Murray, and A. D. Yoffe, *J. Phys. C* **5**, 759 (1972).
 [2] T. Boker, R. Severin, A. Müller, C. Janowitz, R. Manzke, D. Voss, P. Kruger, A. Mazur, and J. Pollmann, *Phys. Rev. B* **64**, 235305 (2001).
 [3] K. F. Mak, C. Lee, J. Hone, J. Shan, and T. F. Heinz, *Phys. Rev. Lett.* **105**, 136805 (2010).
 [4] A. Splendiani *et al.*, *Nano Lett.* **10**, 1271 (2010).
 [5] B. Radisavljevic, A. Radenovic, J. Brivio, V. Giacometti, and A. Kis, *Nat. Nanotechnol.* **6**, 147 (2011).
 [6] Y. J. Zhang, J. T. Ye, Y. Matsushashi, and Y. Iwasa, *Nano Lett.* **12**, 1136 (2012).
 [7] Q. H. Wang, K. Kalantar-Zadeh, A. Kis, J. N. Coleman, and M. S. Strano, *Nat. Nanotechnol.* **7**, 699 (2012).
 [8] W. Bao, X. Cai, D. Kim, K. Sridhara, and M. S. Fuhrer, *Appl. Phys. Lett.* **102**, 042104 (2013).

- [9] J. Lee, K. F. Mak, and Jie Shan, [arXiv:1508.03068](https://arxiv.org/abs/1508.03068).
- [10] Z. Y. Zhu, Y. C. Cheng, and U. Schwingenschlogl, *Phys. Rev. B* **84**, 153402 (2011).
- [11] D. Xiao, G.-B. Liu, W. Feng, X. Xu, and W. Yao, *Phys. Rev. Lett.* **108**, 196802 (2012).
- [12] A. Kormanyos, V. Zolyomi, N. D. Drummond, P. Rakyta, G. Burkard and V. I. Falko, *Phys. Rev. B* **88**, 045416 (2013).
- [13] F. Zahid, L. Liu, Y. Zhu, J. Wang, and H. Guo, *AIP Adv.* **3**, 052111 (2013).
- [14] E. Cappelluti, R. Roldan, J. A. Silva-Guillen, P. Ordejon, and F. Guinea, *Phys. Rev. B* **88**, 075409 (2013).
- [15] X. Xu, W. Yao, D. Xiao, and T. F. Heinz, *Nat. Phys.* **10**, 343 (2014).
- [16] J. T. Ye, Y. J. Zhang, R. Akashi, M. S. Bahramy, R. Arita, and Y. Iwasa, *Science* **338**, 1193 (2012).
- [17] K. Taniguchi, A. Matsumoto, H. Shimotani, and H. Takagi, *Appl. Phys. Lett.* **101**, 042603 (2012).
- [18] W. Shi, J. T. Ye, Y. Zhang, R. Suzuki, M. Yoshida, J. Miyazaki, N. Inoue, Y. Saito, and Iwasa, *Sci. Rep.* **5**, 12534 (2015).
- [19] J. M. Lu, O. Zeliuk, I. Leermakers, N. F. Q. Yuan, U. Zeitler, K. T. Law, and J. T. Ye, *Science* **350**, 1353 (2015).
- [20] Y. Saito *et al.*, *Nat. Phys.* **12**, 144 (2016).
- [21] X. Xi, L. Zhao, Z. Wang, H. Berger, L. Forro, J. Shan, and K. F. Mak, *Nat. Nanotechnol.* **10**, 765 (2015).
- [22] X. Xi, Z. Wang, W. Zhao, J. Park, K. T. Law, H. Berger, L. Forro, J. Shan, and K. F. Mak, *Nat. Phys.* **12**, 139 (2016).
- [23] Y. Ge and A. Y. Liu, *Phys. Rev. B* **87**, 241408(R) (2013).
- [24] R. Roldan, E. Cappelluti, and F. Guinea, *Phys. Rev. B* **88**, 054515 (2013).
- [25] M. Rosner, S. Haas, and T. O. Wehling, *Phys. Rev. B* **90**, 245105 (2014).
- [26] N. F. Q. Yuan, K. F. Mak, and K. T. Law, *Phys. Rev. Lett.* **113**, 097001 (2014).
- [27] L. P. Gor'kov and E. I. Rashba, *Phys. Rev. Lett.* **87**, 037004 (2001).
- [28] P. A. Frigeri, D. F. Agterberg, A. Koga, and M. Sigrist, *Phys. Rev. Lett.* **92**, 097001 (2004).
- [29] See Supplemental Material at <http://link.aps.org/supplemental/10.1103/PhysRevB.93.180501> for pairing correlations with spin-triplet order parameters; tight-binding model parameters; comparison between Ising superconductors and Rashba superconductors.
- [30] P. A. Frigeri, D. F. Agterberg, and M. Sigrist, *New J. Phys.* **6**, 115 (2004).
- [31] J. Liu, A. C. Potter, K. T. Law, and P. A. Lee, *Phys. Rev. Lett.* **109**, 267002 (2012).
- [32] N. F. Q. Yuan, Y. Lu, J. J. He, and K. T. Law, [arXiv:1510.03137](https://arxiv.org/abs/1510.03137).
- [33] X. W. Li, A. Gupta, and G. Xiao, *Appl. Phys. Lett.* **75**, 713 (1999).
- [34] E. Goering, A. Bayer, S. Gold, G. Schutz, M. Rabe, U. Rudiger, and G. Guntherodt, *Phys. Rev. Lett.* **88**, 207203 (2002).
- [35] M. Z. Hasan and C. L. Kane, *Rev. Mod. Phys.* **82**, 3045 (2010).
- [36] X. L. Qi and S. C. Zhang, *Rev. Mod. Phys.* **83**, 1057 (2011).
- [37] J. Alicea, *Rep. Prog. Phys.* **75**, 076501 (2012).
- [38] C. W. J. Beenakker, *Annu. Rev. Condens. Matter Phys.* **4**, 113 (2013).
- [39] J. D. Sau, R. M. Lutchyn, S. Tewari, and S. Das Sarma, *Phys. Rev. Lett.* **104**, 040502 (2010).
- [40] J. Alicea, *Phys. Rev. B* **81**, 125318 (2010).
- [41] Y. Oreg, G. Refael, and F. von Oppen, *Phys. Rev. Lett.* **105**, 177002 (2010).
- [42] P. A. Lee, [arXiv:0907.2681](https://arxiv.org/abs/0907.2681).
- [43] M. Sato and S. Fujimoto, *Phys. Rev. B* **79**, 094504 (2009).
- [44] A. C. Potter and P. A. Lee, *Phys. Rev. Lett.* **105**, 227003 (2010).
- [45] V. Mourik, K. Zuo, S. M. Frolov, S. R. Plissard, E. P. A. M. Bakkers, and L. P. Kouwenhoven, *Science* **336**, 1003 (2012).
- [46] M. T. Deng, C. L. Yu, G. Y. Huang, M. Larsson, P. Caroff, and H. Q. Xu, *Nano Lett.* **12**, 6414 (2012).
- [47] A. Das, Y. Ronen, Y. Most, Y. Oreg, M. Heiblum, and H. Shtrikman, *Nat. Phys.* **8**, 887 (2012).
- [48] S. Nadj-Perge, I. K. Drozdov, J. Li, H. Chen, S. Jeon, J. Seo, A. H. MacDonald, B. A. Bernevig, and A. Yazdani, *Science* **346**, 602 (2014).
- [49] A. Y. Kitaev, *Phys. Usp.* **44**, 131 (2001).
- [50] A. P. Schnyder, S. Ryu, A. Furusaki, and A. W. W. Ludwig, *Phys. Rev. B* **78**, 195125 (2008).
- [51] J. Klinovaja and D. Loss, *Phys. Rev. B* **88**, 075404 (2013).